ELF1 upregulates MEIS1 to accelerate proliferation, migration and invasion of glioma cells through the GFI1/FBW7 axis

Meixiong Cheng
Sichuan Provincial People's Hospital
Yi Zeng
Sichuan Provincial People's Hospital
Tian Zhang
Sichuan Provincial People's Hospital
Min Xu
Sichuan Provincial People's Hospital
Yaqiu Wu (wuyaqiu@med.uestc.edu.cn)
Sichuan Provincial People's Hospital https://orcid.org/0000-0002-3191-2745
Zhili Li (2862826488@qq.com)
Sichuan Privincial People's Hospital

Research

Keywords: ELF1, MEIS1, GFI1, Enhancer, Glioma

Posted Date: April 20th, 2020

DOI: https://doi.org/10.21203/rs.3.rs-23088/v1

Abstract

Background: To explore whether the transcription factor ELF1 affects the GFI1-FBW7 through MEIS1, thus participating in the occurrence and development of glioma. In this study, key transcription factors were identified by differential analysis of GEO database, and downstream regulatory pathways were predicted by available literature.

Methods and results: Based on bioinformatics analysis and existing studies, we speculate that the transcription factor ELF1 may regulate FBW7 through MEIS1-mediated GFI1 and thus affect the occurrence of glioma. The expressions of transcription factors ELF1, MEIS1 and GFI1 were up-regulated in glioma tissues, and the prognosis of glioma patients with high expression of ELF1 was worse.We found that interfering with ELF1 expression in glioma cells can reduce the proliferation, migration and invasion of tumor cells and induce cell apoptosis. The results of Western-blot showed that the expressions of PCNA and MMP9 were decreased, while the expression of cleaved caspase-3 was up-regulated. ChIP experiments showed that ELF1 binds to the MEIS1 promoter region, and MEIS1 can activate the enhancer of GFI1. In vivo experiments were carried out in nude mice, the results showed that interfering ELF1 could inhibit tumor growth in nude mice through the MEIS1-GFI1/FBW7.

Conclusion: Therefore, interference of ELF1 in glioma can reduce its ability to recruit the transcription factor MEIS1, and further impair the activation ability of MEIS1 to GFI1 enhancer, which resulting in suppression of proliferation, migration and invasion and induction of cell apoptosis in glioma cells.

Background

Malignant gliomas are among the most common primary brain tumors in adults [1]. Due to the infiltrative nature of this disease and the localization close to eloquent brain areas, surgical resection with a margin of healthy tissue is basically impossible. Consequently, tumor recurrence is inevitable despite best standard of care. Patients diagnosed with a malignant glioma such as glioblastoma face a fierce clinical course with a survival time of less than 2 years for most patients [2, 3]. Based on advances in the molecular characterization of these tumors disease-associated targets including EGFR or VEGFR were identified which led to the development of new approaches using traditional routes of drug development[4–6]. According to the World Health Organization (WHO) classification of tumors of the central nervous system, gliomas can be categorized into four grades (grade I to IV), among which grade IV is also called glioblastoma or glioblastoma multiforme (GBM) [7]. Moreover, a gene expression-based molecular classification of glioblstoma has been presented, including proneural, neural, classical, and mesenchymal subtypes [8]. Despite the identification of these different subtypes, no effective targeted therapy for gliomas has been developed in recent decades to improve outcomes, and most low-grade gliomas (WHO grade I and II) are inevitably recurrent and progress to high-grade gliomas (WHO grade III and IV). Unfortunately, these strategies failed so far, because the complexity of the disease was underestimated and important factors such as the capability of therapeutics to pass the blood-brain barrier or to penetrate the tumor tissue were not sufficiently considered. This perspective is substantiated

by the fact that areas of variant morphology exhibit significant differences in gene expression subtype within a single tumor, yet harbor a large number of identical genetic alterations [9].

ETS family transcription factors play major roles in prostate tumorigenesis with some acting as oncogenes and others as tumor suppressors. ETS factors can compete for binding at some cis-regulatory sequences, but display specific binding at others. Therefore, changes in expression of ETS family members during tumorigenesis can have complex, multimodal effects. Recent research showed that ELF1 could serve as a possible factors for tumor progression[10]. Genome-wide mapping in cell lines indicated that ELF1 has two distinct tumor suppressive roles mediated by distinct cis-regulatory sequences. ELF1 and ELF2, closely related transcription factors to ELF4, also exerted proliferative effect in various cancer cell lines [11]. Furthermore, knockdown of ELF1 increased docetaxel resistance, indicating that the genomic deletions found in metastatic prostate tumors may promote therapeutic resistance through loss of both c1 in glioma can reduce its ability to recruit the transcription factor Myeloid ecotropic viral integration site 1 (MEIS1), and further impair the activation ability of MEIS1 to Growth factor independence 1 (GFI1) enhancer, which resulting in suppression of proliferation, migration and invasion and induction of cell apoptosis in glioma cells [12]. MEIS1 is a transcription factor that regulate important functions in cell fate determination during development and cell proliferation [13]. GFI1 is located within chromosome 1p22 in the human genome, and as a zinc finger protein, GFI1 mainly functions as a transcriptional repressor by direct or functional interaction with other co-factors [14]. The tumor suppressive mechanisms of these normally expressed ETS factors and their interplay with oncogenic ETS factors are not well understood.

In our study, we found interference of ELF1 in glioma can reduce its ability to recruit the transcription factor MEIS1, and further impair the activation ability of MEIS1 to GFI1 enhancer, which resulting in suppression of proliferation, migration and invasion and induction of cell apoptosis in glioma cells.

Materials And Methods

Bioinformatics analysis

|logFC|>1 and P < 0.01 were used as threshold to analyze glioma expression databases GSE12657, GSE35493, GSE104291 and GSE50161 in GEO database (https://www.ncbi.nlm.nih.gov/gds) by R language "limma" package (http://www.bioconductor.org/packages/release/bioc/html/limma.html). Expression database GSE12657 contained a total number of 12 samples, including 5 normal samples and 7 glioma samples. Expression database GSE35493 contained a total number of 19 samples, including 7 normal samples and 12 glioma samples. Expression database GSE104291 contained a total number of 6 samples, including 2 normal samples and 4 glioma samples. Expression database GSE50161 contained a total number of 47 samples, including 13 normal samples and 34 glioma samples. Key genes in these expression databases were obtained by co-expressed analysis through “Robust Rank Aggreg” (https://cran.r-project.org/web/packages/RobustRankAggreg/index.html). HTF target (http://bioinfo.life.hust.edu.cn/hTFtarget#!/) and Cist Rome (http://cistrome.org/) were used to

obtain the names of human transcription factors. The key transcription factors were obtained by comparing the names of key genes and transcription factors, taking the intersection and combing with the existing literature. The possible downstream regulatory pathways were predicted through the existing literature, and the relationship of the downstream pathways was verified by correlation analysis and MEM (https://biit.cs.ut.ee/mem/index.cgi) co-expression analysis.

Sample collection

Sixty of glioma specimens by surgical removal which were confirmed by pathology analysis were collected from January 2014 to January 2015. These selected patients (male, 38, female, 22; aged range 49–71, the average age 61; stage□-□, 31, stage □-□, 29; KPS score > 70, 35, KPS score < 70, 25) were the first time for surgical treatment. Excluded criteria: patients with other malignant tumor concurrent, incomplete clinical information, serious heart disease, kidney disease and lung dysfunction; In addition, 24 cases of normal brain tissues removed by internal decompression surgery due to severe craniocerebral injury were taken as the control group, all of which were not treated with chemoradiotherapy before surgery. Sixty glioma patients were followed up until January 2020 by telephone or follow-up visit. The 3-year OS of each patient was observed. By the end of follow-up, 2 out of 60 patients had lost to follow-up, with a follow-up rate of 96.67%. Follow-up time was 5–36 months. All patients in this study signed the informed consent and were approved by our medical ethics committee to comply with the Helsinki declaration.

Cell culture and transfection

Glioma cell lines A172 and U251 cells provided by Stem Cell Bank, Chinese Academy of Sciences were cultured in 1640 medium containing 10% fetal bovine serum, 100 U/mL penicillin and 100 mg/mL streptomycin at 37℃ in 5% CO_2.

According to the experimental requirements, cells were transfected respectively. When the cell density reached 90% and was in the logarithmic growth phase, cells were digested with trypsin, made into cell suspension (2.5×10^4 cell/mL), and inoculated on 6-well plates (2 mL for each well). Lentiviral vectors were constructed using lv5-gfp (lentiviral gene overexpression Vector), psih1-h1-copgfp siRNA Vector (lentiviral siRNA fluorescence expression Vector gene silencing Vector). Si-ELF1, si-GFI1, oe-MEIS1 and their negative controls were all constructed by Thermo Fisher Scientific (Waltham, MA, USA). Lentivirus was packaged in 293T cells, which were cultured in RPMI-1640 complete medium containing 10% fetal bovine serum and passed every other day. When the A172 and U251 cells were in the logarithmic growth phase, they were digested by trypsin and blown, and 2 mL cell suspensions (1×10^5 cells/mL) were inoculated on 6-well plates, and cultured overnight at 37℃. Then the virus (1×10^8 TU/ml) was added to the cells for infection, and cells with stable heredity were obtained and collected for subsequent experiments. Sequence of si-ELF1: GGATGTTGCTGAAGAAGAA, Sequence of si-gif1: CGAGCAGACAGCACTTCAA.

RT-qPCR

Total RNA (Invitrogen, Car, USA) was extracted according to the instructions of Trizol method, and the RNA was reversely transcribed into cDNA using Prime Script RT kit (RR037A, Takara, Shiga, Japan) with a system of 10 μL. Then the reaction liquid was exposed to fluorescent quantitative PCR based on operate instruction of SYBR® Premix Ex Tag™ □ kit (RR820A, Takara). The samples were subjected to real-time quantitative PCR using a real-time quantitative PCR system (ABI 7500, ABI, Foster City, CA, USA). With GAPDH as internal control, the 2 - ΔΔ Ct method was used to calculate the relative gene expression. Relevant primers were assigned to Shanghai Sangon Biotech (Shanghai, China) (Table 1).

Protein extraction and quantification

About 1×10^6 cells were treated with 1 ml cell lysate (containing protease inhibitor) (P0013J, Bey time biotechnology CO., LTD., Shanghai, China) for 45 min, and then cleaved for 30 min at 4℃ and 8000 rpm to collect the supernatant. And the protein concentration of each sample was determined using the BCA kit (PC0020, Beijing Solebar biotechnology CO., LTD., Beijing, China). After electrophoresis, the proteins were transferred to a nitrocellulose membrane (66485, PALL, NY, USA). After membrane transformation, the membrane was blocked in 5% skim milk at room temperature for 2 h, and washed with trimethyl aminomethane buffer brine (TBS/T) for 3 times, each time for 10 min. The membrane was incubated with the primary antibodies ELF1 (ab64937, 1:500, Abcam, USA), MEIS1 (ab19867, 1:1000, Abcam, USA), GFI1 (ab21061, 1:1000, Abcam, USA), MMP2 (ab92536, 1:1000, Abcam, USAUSA), PCNA (ab92552, 1:1000, Abcam, USA), Caspase 3 (ab13847, 1:500, Abcam, USA), cleaved-caspase 3 (ab32042, 1:500, Abcam, USA) and GAPDH (ab9485, 1:1000, Abcam, USA). The next day, the membrane was washed at room temperature with TBS/T for 3 times, each time for 5 min. Horseradish peroxidase (HRP)-labeled goat anti-rabbit IgG (ab97051, 1:2000, Abcam, USA) was added and incubated at room temperature for 1 h. The membrane was washed with TBS/T for 10 min × 3 times, immersed in ECL reaction solution (BM101, Bioimage, USA) for 1 min, and then exposed with X-ray in the dark, and finally the target protein bands were measured. GAPDH was used as internal parameter, and the ratio of gray value of target band and internal reference band was used as the relative expression of protein.

Cell proliferation assay

After transfection, A172 and U251 cells were digested and resuscitated. The cell concentration was adjusted to 1×10^5 cells/mL, and the cells were inoculated into a 96-well plate with 100 μL/well and routinely cultured overnight. Cells were treated according to the instructions of CCK-8 kit (Beyotime, Shanghai, China), and cell viability was measured by CCK-8 at 24, 48, 72, and 96 h after inoculation. At each test, 10 μL of CCK-8 detection solution was added, incubated in the incubator for 4 h, and absorbance at 450 nm was tested with an enzyme marker, and the growth curve was drawn.

Cell invasion ability experiment

In the transwell invasion experiment, the Matrigel stored at -80℃ was melted into a liquid overnight at 4℃. And 200 μL of Matrigel was added to 200 μL of serum-free medium. And then 50 μL of Matrigel were added to upper chamber and incubated for 2–3 h until the gel became solid. Cells were digested and counted, and cell suspension was prepared with serum-free medium. Next, 200 μL cell suspension was

added to the upper chamber of each well, and 800 μL cell suspension was added to the lower chamber containing 20% FBS conditioned medium. Cells were incubated at 37℃ for 20–24 h. After that, transwell plate was soaked in formaldehyde for 10 min, and rinsed with pure water for 3 times. The cells were stained with 0.1% crystal violet at room temperature for 30 min, and the cells on the upper surface were wiped off with cotton balls. Cells on the membrane were observed, photographed and counted by an inverted microscope. Substrate glue was not required for transwell migration experiment, and the incubation time was 16 h. Cells from at least four randomly selected microscope regions were counted.

Cell apoptosis assay

After transfection for 48 h, the cells were digested with 0.25% trypsin and collected in the flow tube, centrifuged, and the supernatant was discarded. Annexin-V-FITC, PI, and HEPES buffer were incorporated into annexin-V-FITC/PI dye at a ratio of 1:2:50 according to the instructions of Annexin-V-FITC apoptosis assay kit (559763, Becton, Dickinson and Company, NY, USA). And 1×10^6 cells were resuspended in 100 μL of dye solution, and the cells were oscillated and mixed. After incubation at room temperature for 15 min, 1 mL HEPES buffer (PB180325, Porcello, Wuhan, China) was added to the solution for oscillating and mixing. FITC and PI fluorescence were detected by excitation of 525 nm and 620 nm bandpass filters at the wavelength of 488 nm to detect cell apoptosis.

Chromatin immuno-coprecipitation (ChIP)

The EZ-Magna ChIP kit (EMD Millipore) was used for ChIP determination. According to the manufacturer's protocol, the cells were immobilized with 4% paraformaldehyde and incubated with glycine for 10 min to produce DNA-protein cross-linking. The cells were then lysed with a cell lysis buffer and a nuclear lysis buffer and treated with ultrasound to produce 200–300 bp of chromatin fragments (a portion of the DNA as INPUT). Next, lysates were immunoprecipitated by magnetic protein A beads antibodies bonded with various antibodies. H3K27ac antibody (ab177178, Abcam, USA) or H3K4me1 (ab176877, Abcam, USA) were added to the target protein group. Negative control was added with rabbit IgG (ab171870, Abcam, USA; RRID). Finally, the precipitated DNA was analyzed by RT-qPCR.

In vivo animal experiment

Ten BALB/c male nude mice (age: 4–5 weeks old; weight: 18–22 g) were purchased from Shanghai SLAC Laboratory Animal Co., Ltd. (Shanghai, China). Si-ELF1 was used to construct lentivirus vector to obtain stable interference expression of ELF1 and negative control of human U251 cell line. Cell suspension (20 μL, 1.0×10^6 cells/mL) was inoculated in nude mice at abdominal subcutaneous. Tumors were observed weekly and measured with vernier caliper. Calculation formula of tumor volume (TV) is: $TV = 1/2 * a * b^2$, where a is length of tumor and b is width of tumor. Mice were exposed to euthanasia at 35 d, and tumors of each groups were removed, weighted and photographed. All the above experimental animals have been approved by the animal protection and use committee, and all the animal experiments in this study are in accordance with the management and use principles of local experimental animals.

Immunohistochemistry

Paraffin-embedded tumor tissues were subjected to dewaxing, hydration, xylene I, II dewaxing, and gradient alcohol dehydration. Sections were immersed in 3% H_2O_2 for 10 min, washed with PBS twice for 5 min and repaired with antigen (Beyotime, Shanghai, China) at high pressure for 90 s, and then cooled down at room temperature. Sections were blocked with 5% BSA at 37℃ for 30 min, and incubated with primary rabbit antibody at 4℃ overnight. Then tissues were incubated with HRP labeled goat anti rabbit (ab205718, 1: 1000Abcam) at 37℃ for 30 min. Finally, sections were exposed to DBA solution (MXB, Fuzhou, China), stained with hematoxylin for 5 min, and observed by optical microscope (XSP-36, BSD., Shenzhen, China) and photographed. Five high-power fields were randomly selected from each section, and 200 cells were counted in each field. The number of positive cells < 5% was negative, and the number of positive cells ≥ 5% was positive. The immunohistochemical results were scored by two people independently using double-blinded fashion.

Statistical analysis

All the present data were expressed as mean ± standard deviation of three independent experiments. The significant difference from the respective control for each experimental test was assessed by one-way analysis of variance (ANOVA) using SPSS21.0 software (IBM Corp, Armonk, NY, USA). The difference is considered significant if $p < 0.05$.

Results

ELF1 is highly expressed in glioma tissues and correlates with WHO grading and KPS score of patients

GEO databases GSE12657, GSE35493, GSE104291 and GSE50161 were analyzed by R language, and we found 1507, 4173, 2784 and 4554 significantly differentially expressed glioma genes respectively. We found that there were 578 genes expressed in these four expression databases through coexpression analyzing using "RobustRankAggreg" pack (Fig. 1A). We select eight key transcription factors by analyzing database of hTFtarget and Cistrome Fig. 1B, the existing literature shows that the ELF1 related to the occurrence of a glioma. From the expression data of expression database GSE35493, we drew a boxplot to determine its significantly high expression in glioma (Fig. 1C).

In order to determine whether ELF1 was involved in the occurrence and development of glioma, the expression of ELF1 in brain tissues of glioma patients was detected by RT-qPCR. Compared with the normal group, the expression of ELF1 in glioma tissues was significantly increased (Fig. 1D). The expression of ELF1 increased with the increase of WHO grade of glioma ($p < 0.05$) (Fig. 1E). In addition, we analyzed the ELF1 expression and the link between the patient clinical pathological features.

According to the ELF1 average expression in gliomas (1.56), it was divided into high and low expression group. The results showed that the expression of ELF1 had an obvious correlation with the WHO classification and KPS scores in patients, however, there was no significant correlation between expression of ELF1 and patient's age, gender, tumor size and tumor recurrence (Table.2). After Kaplan Meier analysis, the Logrank test of survival data showed that expression of ELF1 was negatively correlated with survival time and prognosis of patients (Fig. 1F).

Silencing ELF1 inhibits the proliferation, migration and invasion of glioma cells and promotes cell apoptosis

In view of the significant upregulation of ELF1 in glioma tissues, in order to determine how it affected the proliferation, migration and invasion ability of glioma cells, we first constructed siRNA specific to ELF1. After transfection with si-ELF1, the expression of ELF1 was significantly decreased in glioma cells A172 and U251 according to results of RT-qPCR and Western-blot (Fig. 2A). From results of CCK8, transwell assay and Annexin V/PI dual staining, glioma cells abilities of proliferation, migration and invasion were significantly inhibited and cells apoptosis was induced after interference of ELF1 (Fig. 2B-D). Proliferation-related factor PCNA, invasion-related factor MMP2, and apoptosis-related factor Cleaved caspase-3 expression was detected by Western-blot, and results showed that compared with the si-NC group, expressions of PCNA and MMP2 in the si-ELF1 group were significantly decreased, while expressions of Cleaved caspase-3 were significantly increased (Fig. 2F).

Transcription factor ELF1 binds to the MEIS1 promoter to promote its transcription and promote the development of glioma.

In the above studies, we have identified that ELF1 was highly expressed in glioma tissues and can significantly inhibit the proliferation, migration and invasion of glioma cells after specific interference treatment. And then we continue our review of relevant literature, and found ELF1, a transcription factor, can be combined into MEIS1 promoter regions, thus affect the transcription [15]. We used the expression database GSE50161 expression data calculated ELF1 and MEIS1 identified a significant correlation between the relevance of the (Fig. 3A), and fond that MEIS1 was significant highly expressed in glioma tissues according to the expression database GSE35493 (Fig. 3B). We hypothesized that ELF1 may affect glioma development by regulating the transcription of MEIS1. So we first detected MEIS1 expression in glioma and normal control tissues through the RT-qPCR, and the results showed that compared to normal brain tissues, the expression of glioma tissues MEIS1 rise significantly (Fig. 3C). Then, based on the ChIP experiments, we verified a fact that (Fig. 3D) compared with the IgG group, the promoter DNA of binding MEIS1 in ELF1 group was significantly increased. When si-ELF1 was transfected into glioma cells, mRNA and protein expressions of MEIS1 were significantly decreased (Fig. 3E).

Furthermore, to determine whether ELF1 involved in the development of glioma through affecting the transcription of MEIS1, we transfected si-NC + oe-NC, si-ELF1 + oe-NC and si-ELF1 + oe-MEISL into glioma cells A172 and U251, respectively, to observe their effects on cell proliferation, migration, invasion and apoptosis. In the si-ELF1 + oe-NC group, cell proliferation, migration and invasion ability were significantly reduced, and cell apoptosis rate was significantly up-regulated in comparison with the control group. However, when transfected with si-ELF1 + oe-MEISL at the same time, results showed that overexpression of MEIS1 reversed the effect of ELF1 interference on glioma cells, promoting the growth, migration and invasion of glioma cells, and reducing cell apoptosis (Fig. 3F-I).

Western-blot revealed that expression of PCNA and MMP2 in the si-ELF1 + oe-NC group was decreased and the expression of Cleaved caspase-3 was increased compared with the si-NC + oe-NC group, when oe-MEISL was added, the expression of PCNA and MMP2 was up-regulated, while that of Cleaved caspase-3 was decreased (Fig. 3J). These results suggested that the transcription factor ELF1 may be involved in glioma development by enhancing MEIS transcription in glioma.

MEIS1 promotes glioma development by regulating the activity of GFI1 enhancer

After MEM analysis, we found that there existed co-expression relationship between MEIS1 and GFI1 (Fig. 4A). We then tested GFI1 expression in the glioma and normal control tissues by RT-qPCR, and results showed that expression of GFI1 in glioma tissues was higher (Fig. 4B). Moreover, after the overexpression of MEIS1 in glioma cells, GFI1 expression was detected by Western-blot. The results showed that the overexpression of MEIS1 in glioma cells would promote the expression of GFI1 (Fig. 4C). Then the ChIP experiment was used to verify the relationship between MEIS1 and GFI1. The results showed that after overexpression of MEIS1 in A172 and U251 cells, the enrichment of H3K4me1, H3K27ac and MEIS1 in the GFI1 enhancer region, as well as the promoter region of GFI1, H3K4me3, H3K27ac and GFI1 increased significantly. These results indicated that MEIS1 promoted the expression of GFI1 by activating the enhancer of GFI1 (Fig. 4D-E).

To make it clear that MEIS promotes glial development by regulating GFI1, we overexpressed MEIS or interfered GFI1 in U251 cells, and overexpressed MEIS and interfered GFI1 expression simultaneously. We continued to detect cell proliferation by CCK-8, migration and invasion by transwell, and apoptosis by flow cytometry. The results showed that, compared with the oe-NC + si-NC group, cell proliferation, migration and invasion were up-regulated while apoptosis rate was decreased in the oe-MEIS1 + si-NC group. Moreover, after overexpressing MEIS1, the cells were treated with GFI1 interference. The results showed that oe-MEIS1 + si-GFIL reversed the effect of overexpressing MEIS1 (Fig. 4F-I). Furthermore, Western-blot was used to detect the expression of cell proliferation, migration, invasion and apoptosis-related proteins in each group. As displayed in Fig. 4J, interference with GFI1 could reverse the effect of overexpression of MEIS1 on all related proteins, inhibited the expression of PCNA and MMP2, and promoted the expression of Cleaved caspase-3.

In the occurrence of cervical cancer, it has been reported that GFI1 can inhibit the expression of FBW7 through its correlation with FBW7 [16]. By calculating the correlation between GFI1 and FBW7 (FBXW7 included in NCBI) on expression database GSE50161, it was found that there was a significant negative correlation (Fig. 4K). Through the expression database GSE35493, we found that FBW7 was significantly poorly expressed in glioma (Fig. 4L). GFI1 and FBW7 had a significantly co-expressed relationship, as evidenced by MEM analysis (Fig. 4M). In addition, we continue to detect the expression of FBW7 in glioma cells by Western-blot after transfection with MEIS1or GFI1. As shown in Fig. 4N, compared with the oe-NC + si-NC group, FBW7 expression was significantly lower in the oe-MEIS1 + si-NC group. When co-transfected with oe-MEIS1 + si-GFI1, expression of FBW7 had no significant change. These results suggested that by MEIS1 could upregulate the activity of GFI1 enhancer, followed by inhibiting expression of FBW7 and then promoted the proliferation, migration, invasion and inhibited apoptosis of glioma cells.

Interference with ELF1 can inhibit glioma progression in vivo by MEIS1/GFI1/FBW7 axis

In order to confirm the anti-tumor effect of ELF1 *in vivo*, we established a mouse model of xenotransplantation and inoculated U251 cells (interference of ELF1) into mice. The results showed that the growth and weight of tumor in mice treated with si-ELF1 were lower than those in the control group (Fig. 5A-C). In addition, Western-blot analysis showed that si-ELF1 treatment significantly reduced the expression of ELF1, MEIS1 and GFI1, and promoted the expression of FBW7 (Fig. 5D). These results indicated that interference with ELF1 would inhibit MEIS1/GFI1, thereby promoting expression of FBW7 and retarding tumor growth *in vivo*.

Discussion

Gliomas comprise the most common type of primary malignant brain tumor, and except for pilocytic astrocytoma and subependymal giant cell astrocytoma, nearly all are characterized by a high recurrence rate, a lack of effective treatment strategies, high rates of mortality, and short survival times. Only 5.5% of patients typically survive 5 years postdiagnosis and the median overall survival is still dismal at approximately 14.5–16.6 months even with multimodal therapy comprised of surgery, radiotherapy, and chemotherapy [8]. In the present study, we demonstrated that interference of ELF1 in glioma can reduce its ability to recruit the transcription factor MEIS1, and further impair the activation ability of MEIS1 to GFI1 enhancer, which resulting in suppression of proliferation, migration and invasion and induction of cell apoptosis in glioma cells.

ELF1 was identified as a potential downstream target of the DNA damage response pathway, and following ionizing radiation U2OS cells with a siRNA against ELF1 were more likely to escape cell cycle arrest by bypassing the G2-M checkpoint [17–19]. For the purpose of determining whether ELF1 was

involved in the occurrence and development of glioma, we measured the expression of ELF1 in brain tissues of glioma patients and fond that ELF1 is highly expressed in glioma tissues and closely correlates with WHO grading and KPS score of patients. Therefore, we hypothesized that ELF1 might serve as a factor of tumor promotion. In order to verify our hypothesis, we silenced the ELF1 in A172 and U251 cell lines and found that the proliferation activity of cells was significantly decreased. Additionally, silencing of ELF1 dramatically triggered apoptosis in both A172 and U251 cell lines. Furthermore, activities of migration and invasion of glioma cells were distinctly impaired by silencing of ELF1. The proliferation-related factor PCNA and invasion-related factor MMP2 were downregulated, while apoptosis-related factor cleaved caspase-3 was upregulated after interference of ELF1 in glioma cells. Above results suggested that silencing ELF1 inhibits the proliferation, migration and invasion and promotes cell apoptosis of glioma cells.

MEIS1 is a transcription factor that regulate important functions in cell fate determination during development and cell proliferation [13]. MEIS1 has a key role in regulation of stemness state of stem cells, transcription adjustment of self-renewal genes, as well as involved genes in cell development and differentiation, playing an oncogenic role in several tumors [20]. It is reported that ELF1 can act as an important positive transcriptional regulator of the Hox cofactor MEIS1 [15]. So, we hypothesized that ELF1 may affect glioma development by regulating the transcription of MEIS1. From results of RT-qPCR, the expression of MEIS1 in glioma tissues was significantly upregulated in comparison to normal tissues. In addition, overexpression of MEIS1 reversed the effect of ELF1 interference on promoting the growth, migration and invasion of glioma cells, and reducing cell apoptosis in glioma cells. we can conclude that transcription factor ELF1 may be involved in promoting glioma progression by regulating MEIS1 transcription.

The GFI1 gene, is a zinc finger transcription factor essential for development of the erythroid and megakaryocytic lineages was originally discovered in the hematopoietic system, where it functions as a key regulator of stem cell homeostasis, as well as development of the erythroid and megakaryocytic lineages [21, 22]. Previous study demonstrated that GFI1 expression is controlled by five distinct regulatory regions spread over 100 kilobases, with Scl/Tal1 and MEIS1 acting as upstream regulators in early hematopoietic cells [22]. To elucidate the underlying mechanism between GFI1 and MEIS1 in glioma development, MEM analysis was performed to revealed that there existed significant relationship of co-expression between MEIS1 and GFI1. Overexpression of MEIS1 in glioma cells would significantly increase the enrichment of H3K4me1, H3K27ac and MEIS1 in the GFI1 enhancer region, as well as the promoter region of GFI1, H3K4me3, H3K27ac and GFI1, suggesting that MEIS1 promoted the expression of GFI1 by activating the enhancer of GFI1. Overexpression of MEIS1 would activate the enhancer of GFI1, and then inhibited proliferation, migration and triggered apoptosis in glioma cells. Moreover, study showed that tumor suppressor F-box/WD repeat-containing protein 7 (FBW7), an E3 ubiquitin ligase that mediates ubiquitination and degradation of oncoproteins [23] participated the promoted function of MEIS1/GFI1 in glioma cells. MEIS1 could upregulate the activity of GFI1 enhancer, followed by inhibiting expression of FBW7 and then promoted the proliferation, migration and invasion and suppressed apoptosis of glioma cells.

Finally, subcutaneous tumor mouse model of U251 cells (interference of ELF1) was established to confirm the anti-tumor effect of ELF1 *in vivo*. The results showed that the growth and weight of tumor in mice treated with si-ELF1 were significantly lower than that in the control group. Additionally, compared with control group, downregulated expressions of ELF1, MEIS1 and GFI1, and upregulated expression of FBW7 were found in tumor tissues treated with si-ELF1. The results showed that interference with ELF1 would inhibit MEIS1/GFI1, thereby promoting expression of FBW7 and retarding glioma growth *in vivo*.

Conclusions

In summary, the present study demonstrated that upregulated expression of ELF1 in glioma tissues promoted tumor progression by regulating MEIS1/GFI1/FBW7 axis, suggesting that ELF1 could serve as a promising therapeutic target for glioma.

Abbreviations

WHO: World Health Organization; GBM: glioblastoma multiforme; MEIS1: Myeloid ecotropic viral integration site 1; GFI1: Growth factor independence 1; TBS/T: trimethyl aminomethane buffer brine; HRP: Horseradish peroxidase; ChIP: chromatin immuno-coprecipitation

Declarations

Acknowledgements

We would like to show our sincerest appreciation to the reviewers and their critical comments on this article.

Authors' contributions

Meixiong Cheng, Yi Zeng and Tian Zhang wrote the paper and conceived and designed the experiments; Min Xu and Yaqiu Wu analyzed the data; Yaqiu Wu and Zhili Li collected and provided the sample for this study. All authors have read and approved the final submitted manuscript.

Funding

None.

Availability of data and materials

Data sharing not applicable to this article as no datasets were generated or analysed during the current study.

Ethics approval and consent to participate

All patients in this study signed the informed consent and were approved by our medical ethics committee to comply with the Helsinki declaration.

Consent for publication

Not applicable.

Competing interests

The authors declare no competing interest.

Author details

[1] Department of Neurosurgery, Sichuan Provincial People's Hospital (School of Medicine, University of Electronic Science and Technology of China), Chengdu 610072, P. R. China

[2] Department of Neurosurgery Critical Care Medicine, Sichuan Provincial People's Hospital (School of Medicine, University of Electronic Science and Technology of China), Chengdu 610072, P. R. China

References

1. Ostrom QT, Gittleman H, Truitt G, Boscia A, Kruchko C, Barnholtz-Sloan JS. CBTRUS Statistical Report: Primary Brain and Other Central Nervous System Tumors Diagnosed in the United States in 2011–2015. Neuro Oncol. 2018;20:iv1–86.
2. Oike T, Suzuki Y, Sugawara K, Shirai K, Noda SE, Tamaki T, et al. Radiotherapy plus concomitant adjuvant temozolomide for glioblastoma: Japanese mono-institutional results. PLoS One. 2013;8:e78943.
3. Lesueur P, Lequesne J, Grellard JM, Dugue A, Coquan E, Brachet PE, et al. Phase I/IIa study of concomitant radiotherapy with olaparib and temozolomide in unresectable or partially resectable glioblastoma: OLA-TMZ-RTE-01 trial protocol. BMC Cancer. 2019;19:198.
4. Chinot OL, Wick W, Mason W, Henriksson R, Saran F, Nishikawa R, et al. Bevacizumab plus radiotherapy-temozolomide for newly diagnosed glioblastoma. N Engl J Med. 2014;370:709–22.
5. Gilbert MR, Dignam JJ, Armstrong TS, Wefel JS, Blumenthal DT, Vogelbaum MA, et al. A randomized trial of bevacizumab for newly diagnosed glioblastoma. N Engl J Med. 2014;370:699–708.
6. Boxerman JL, Zhang Z, Safriel Y, Rogg JM, Wolf RL, Mohan S, et al. Prognostic value of contrast enhancement and FLAIR for survival in newly diagnosed glioblastoma treated with and without bevacizumab: results from ACRIN 6686. Neuro Oncol. 2018;20:1400–10.
7. Rogers TW, Toor G, Drummond K, Love C, Field K, Asher R, et al. The 2016 revision of the WHO Classification of Central Nervous System Tumours: retrospective application to a cohort of diffuse gliomas. J Neurooncol. 2018;137:181–9.

8. Brat DJ, Scheithauer BW, Fuller GN, Tihan T. Newly codified glial neoplasms of the 2007 WHO Classification of Tumours of the Central Nervous System: angiocentric glioma, pilomyxoid astrocytoma and pituicytoma. Brain Pathol. 2007;17:319–24.
9. Hovelson DH, Udager AM, McDaniel AS, Grivas P, Palmbos P, Tamura S, et al. Targeted DNA and RNA Sequencing of Paired Urothelial and Squamous Bladder Cancers Reveals Discordant Genomic and Transcriptomic Events and Unique Therapeutic Implications. Eur Urol. 2018;74:741–53.
10. Feik E, Schweifer N, Baierl A, Sommergruber W, Haslinger C, Hofer P, et al. Integrative analysis of prostate cancer aggressiveness. Prostate. 2013;73:1413–26.
11. Ando M, Kawazu M, Ueno T, Koinuma D, Ando K, Koya J, et al. Mutational Landscape and Antiproliferative Functions of ELF Transcription Factors in Human Cancer. Cancer Res. 2016;76:1814–24.
12. Budka JA, Ferris MW, Capone MJ, Hollenhorst PC. Common ELF1 deletion in prostate cancer bolsters oncogenic ETS function, inhibits senescence and promotes docetaxel resistance. Genes Cancer. 2018;9:198–214.
13. Bhanvadia RR, VanOpstall C, Brechka H, Barashi NS, Gillard M, McAuley EM, et al. MEIS1 and MEIS2 Expression and Prostate Cancer Progression: A Role For HOXB13 Binding Partners in Metastatic Disease. Clin Cancer Res. 2018;24:3668–80.
14. Lima K, Carlos J, Alves-Paiva RM, Vicari HP, Souza Santos FP, Hamerschlak N, et al. Reversine exhibits antineoplastic activity in JAK2(V617F)-positive myeloproliferative neoplasms. Sci Rep. 2019;9:9895.
15. Xiang P, Lo C, Argiropoulos B, Lai CB, Rouhi A, Imren S, et al. Identification of E74-like factor 1 (ELF1) as a transcriptional regulator of the Hox cofactor MEIS1. Exp Hematol. 2010;38:798–8, 808 e1-2.
16. Cai H, Zhang F, Li Z. Gfi-1 promotes proliferation of human cervical carcinoma via targeting of FBW7 ubiquitin ligase expression. Cancer Manag Res. 2018;10:2849–57.
17. Yao JJ, Liu Y, Lacorazza HD, Soslow RA, Scandura JM, Nimer SD, et al. Tumor promoting properties of the ETS protein MEF in ovarian cancer. Oncogene. 2007;26:4032–7.
18. Madison BJ, Clark KA, Bhachech N, Hollenhorst PC, Graves BJ, Currie SL. Electrostatic repulsion causes anticooperative DNA binding between tumor suppressor ETS transcription factors and JUN-FOS at composite DNA sites. J Biol Chem. 2018;293:18624–35.
19. Matsuoka S, Ballif BA, Smogorzewska A, McDonald ER 3rd, Hurov KE, Luo J, et al. ATM and ATR substrate analysis reveals extensive protein networks responsive to DNA damage. Science. 2007;316:1160–6.
20. Mahmoudian RA, Bahadori B, Rad A, Abbaszadegan MR, Forghanifard MM. MEIS1 knockdown may promote differentiation of esophageal squamous carcinoma cell line KYSE-30. Mol Genet Genomic Med. 2019;7:e00746.
21. Chowdhury AH, Ramroop JR, Upadhyay G, Sengupta A, Andrzejczyk A, Saleque S. Differential transcriptional regulation of meis1 by Gfi1b and its co-factors LSD1 and CoREST. PLoS One. 2013;8:e53666.

22. Wilson NK, Timms RT, Kinston SJ, Cheng YH, Oram SH, Landry JR, et al. Gfi1 expression is controlled by five distinct regulatory regions spread over 100 kilobases, with Scl/Tal1, Gata2, PU.1, Erg, Meis1, and Runx1 acting as upstream regulators in early hematopoietic cells. Mol Cell Biol. 2010;30:3853–63.
23. Cai J, Sun M, Hu B, Windle B, Ge X, Li G, et al. Sorting Nexin 5 Controls Head and Neck Squamous Cell Carcinoma Progression by Modulating FBW7. J Cancer. 2019;10:2942–52.

Tables

Table 1 Primer sequences used for RT-qPCR

Targets	Primer sequence (5'-3')
ELF1	F: 5′-TGTTGTCCAACAGAACGACCT-3′
	R: 5′-GGAAAAATAGCTGGATCACCA-3′
MEIS1	F:5′-TCACACTGGCCTTAAAGAGGA-3′
	R:5′-CCGTAATGGGGTAGATCGTC-3′
GFI1	F: 5'-AGCTGTGTAACACTACCGTGAGGAT-3'
	R:5'-ACCATGATGAGCTTTGCACACT-3'
GAPDH	F:5'-GCACCGTCAAGGCTGAGAAC-3′
	R:5'-TGGTGAAGACGCCAGTGGA-3′

Table 2 The relationship between ELF1 expression and the clinicopathological characteristics of glioma patients

Index	No.	ELF1 expression		P values
		Low expression (n=31)	High expression (n=29)	
Gender				0.431
Male	38	20	18	
Female	22	9	13	
Age				0.793
≥63	35	16	17	
63	25	13	14	
Tumor Diameter				0.795
≥5	33	15	17	
5	27	14	14	
TNM				0.001
I~II	30	28	2	
III~	30	1	29	
KPS				0.001
≥70	35	8	27	
<70	25	21	4	
Relapse				0.062
Yes	37	14	23	
No	23	15	8	

Figures

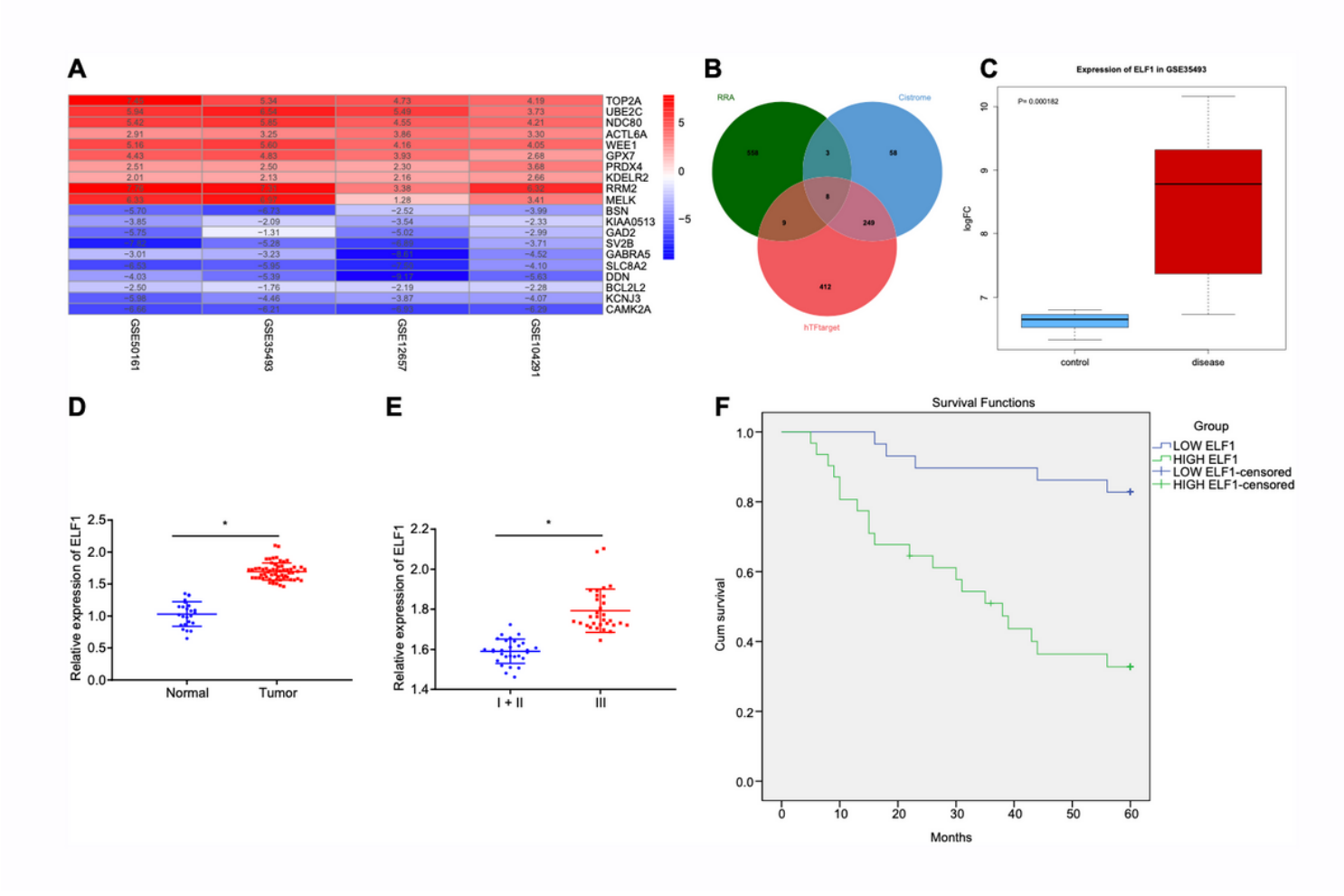

Figure 1

ELF1 is involved in the development of glioma. A: expression heat map of expression databases GSE50161, GSE35493, GSE12657 and GSE104291, the color level of Log FC is on the right side; B: Venn diagram of the intersection of co-expression genes, transcription factors of HTF target and transcription factors of Cist Rome; C: expression data of chip GSE35493 is used to draw the expression boxplot. The blue box on the left represents the expression of normal samples, and the red box on the right represents the expression of glioma samples; D: RT-qPCR analysis of ELF1 expression in glioma tissues and normal control tissues; E: correlation of ELF1 expression and WHO grading in glioma patients; F: Kaplan Meier method to analyze the relationship between ELF1 expression and survival time of patients. * represents $p<0.05$ compared with the normal control tissues, and the above measurement data were expressed as mean ± standard deviation. Un-paired t test was used between the two groups.

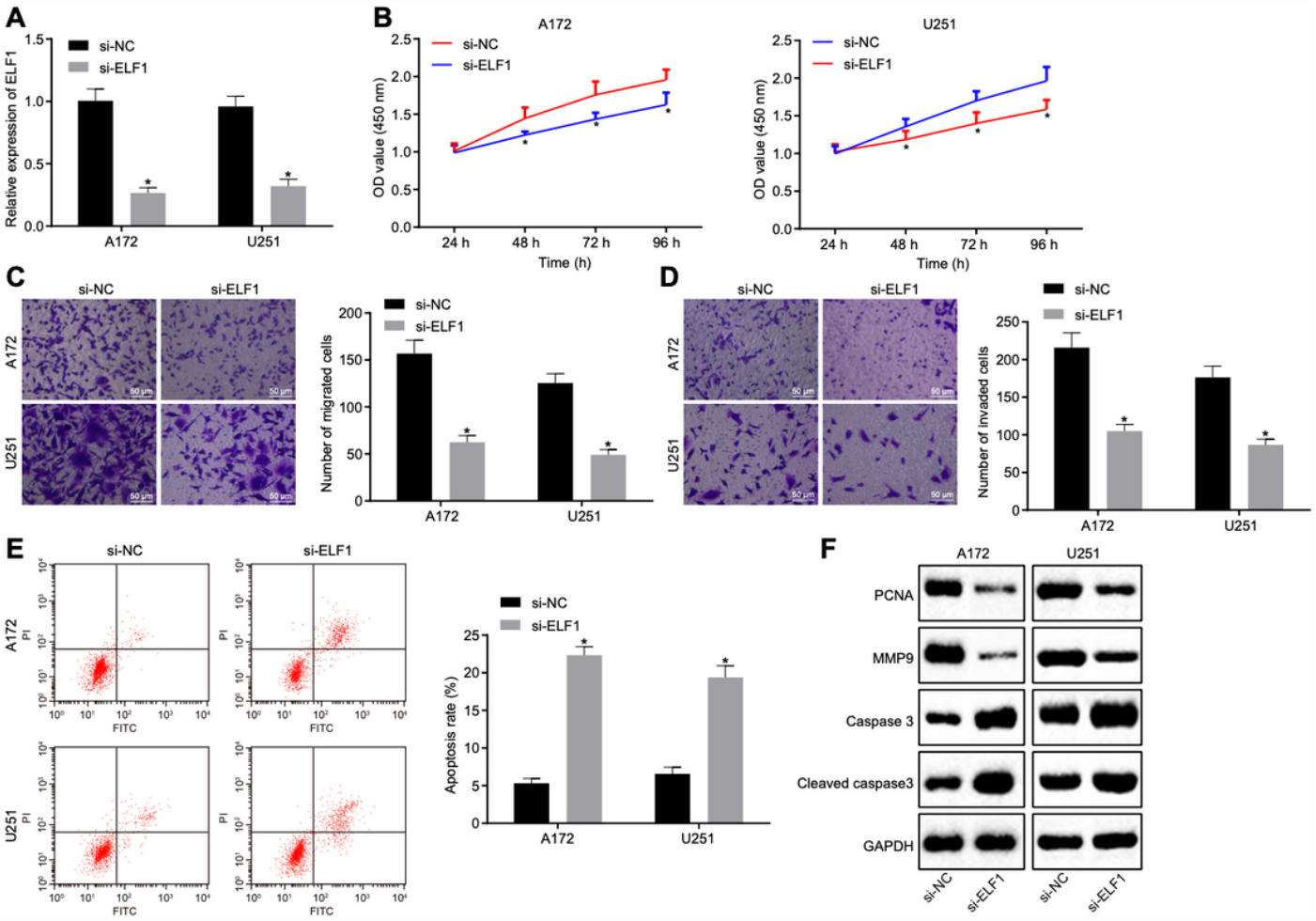

Figure 3

Silencing ELF1 inhibits glioma cell proliferation, migration and invasion, and promotes cell apoptosis. A: expression of interfering ELF1 was tested by RT-qPCR and Western-blot; B: CCK-8 assay was used to detect the inhibited the proliferation of glioma cells; C: interference with ELF1 was detected by transwell to reduce cell migration; D: cell invasion ability decreased after ELF1 interference was used by transwell experiment; E: apoptosis rate of ELF1 cells was used by Annexin-V /PI flow cytometry; F: Western-blot was used to detect the expression of related proteins. * represents $p<0.05$ compared with the si-NC group, and the above values are all measurement data, expressed as mean ± standard deviation. The unpaired t test was used between the two groups, and the data of each group at different time points were compared. The cell experiment was repeated three times.

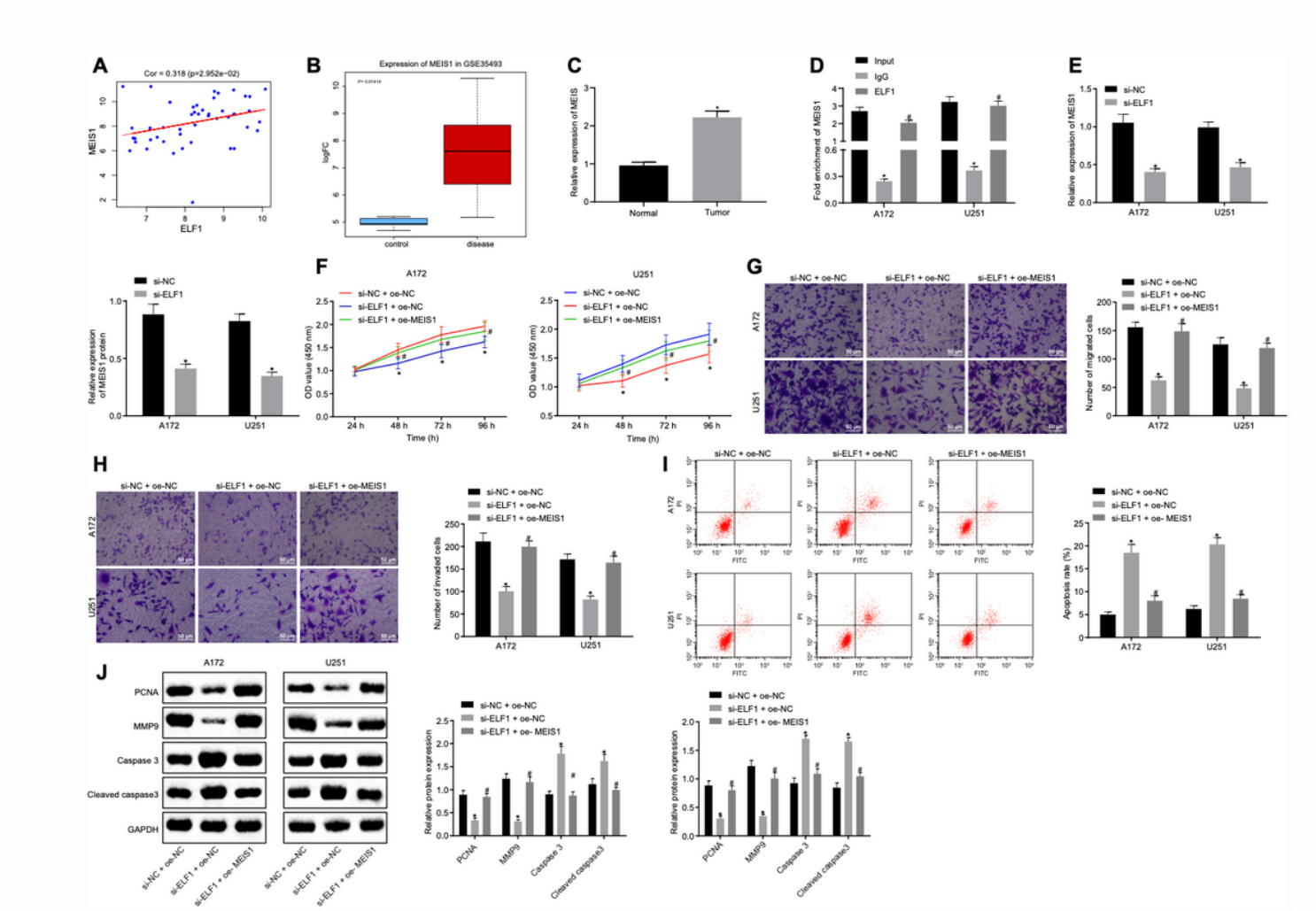

Figure 5

ELF1 binds to the MEIS1 promoter to promote the expression of MEIS1 to participate in the development of glioma. A: the expression correlation diagram of ELF1 and MEIS1 drawn from the expression database GSE50161 data; B: MEIS1 expression box plot drawn from the data of expression database GSE35493. The blue box on the left represents the expression of normal samples, and the red box on the right represents the expression of glioma samples; C; RT-qPCR analysis showed that MEIS1 was significantly up-regulated in glioma tissues; D: ChIP experiment showed that ELF1 was bound to MEIS1 promoter region; E: RT-qPCR and WB results showed significant inhibition of MEIS1 expression after ELF interference; F: CCK-8 assay showed that MEIS1 promoted the proliferation of glioma cells; G: Transwell detected the ability of MEIS1 to promote cell migration; H: Transwell experiment showed that MEIS1 reduced the invasion ability of glioma cells; I: Annexin-V /PI flow showed that MEIS1 inhibited the apoptosis rate of glioma cells; J: Western-blot was used to detect the expression of related proteins. * represents $p<0.05$ compared with Input group and si-NC + oe-NC group, and # represents $p<0.05$ compared with IgG group and si-ELF1+ oe-NC group. The measurement data were expressed as mean ± standard deviation. Un-paired t test was used between the two groups. One-way ANOVA and Tukey's were used for data comparison among multiple groups. The data of each group at different time points were

compared using repeated measure ANOVA and Bonferroni for post-test. The cell experiment was repeated three times.

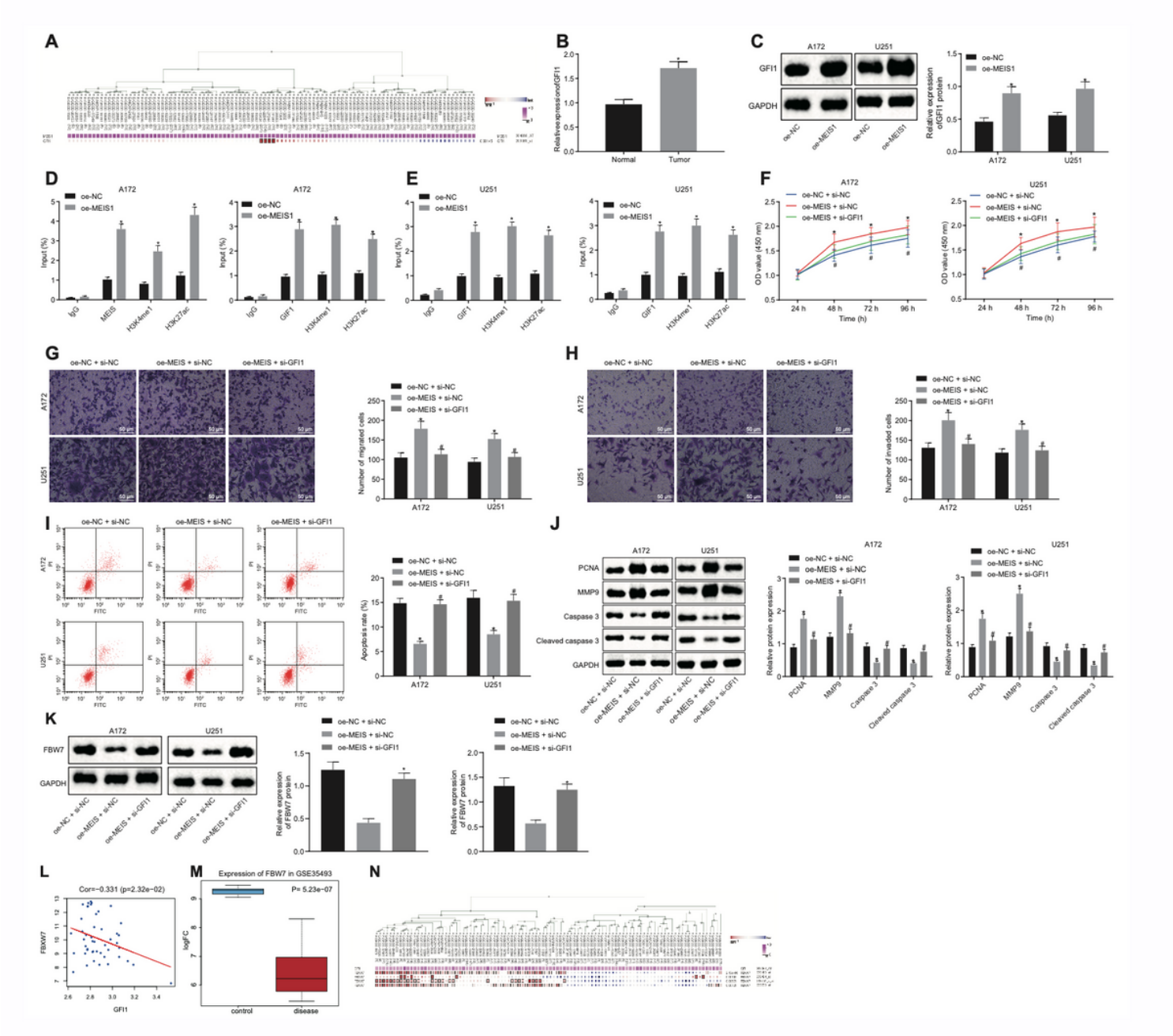

Figure 7

MEIS1 regulates GFI1 enhancer activity in glioma cells. A: MEM analysis showed that there was A significant co-expression relationship between MEIS1 and GFI1; B: RT-qPCR results showed that GFI1 expression was up-regulated in glioma tissues; C: Western-blot showed that MEIS would promote the expression of GFI1; D: ChIP detected the enrichment of H3K4me1, H3K27ac and MEIS1 in the GFI1 enhancer region; E: ChIP detected the enrichment of H3K4me3, H3K27ac and MEIS1 in the promoter region of GFI1; F: interference with GFI1 will inhibit the proliferation of glioma cells; G: interference with GFI1 will inhibit the invasion of glioma cells; H: interference with GFI1 can significantly inhibit glioma cell migration. I: interference with GFI1 significantly promoted the increase of glioma cell apoptosis; J:

Western-blot was used to detect the expression of related proteins after transfection in each cell; K: correlation diagram of GFI1 and FBX7 expression drawn from expression database GSE50161 data; L: the expression boxplot of FBX7 drawn from the expression database GSE35493 data. The blue box on the left represents the expression of normal samples, and the red box on the right represents the expression of glioma sample; M: MEM analysis showed that there was a significant co-expression relationship between GFI1 and FBW7; N: Western-blot was used to detect the expression of FBW7 after transfection in each cell. * represents $p<0.05$. Measurement data were expressed as mean ± standard deviation. Un-paired t test was used between the two groups, and one-way ANOVA and Tukey's were used for post-test for data comparison between multiple groups. Data were compared among groups at different time points by repeated measure ANOVA, and Bonferroni was used for post-hoc test. The cell experiment was repeated three times.

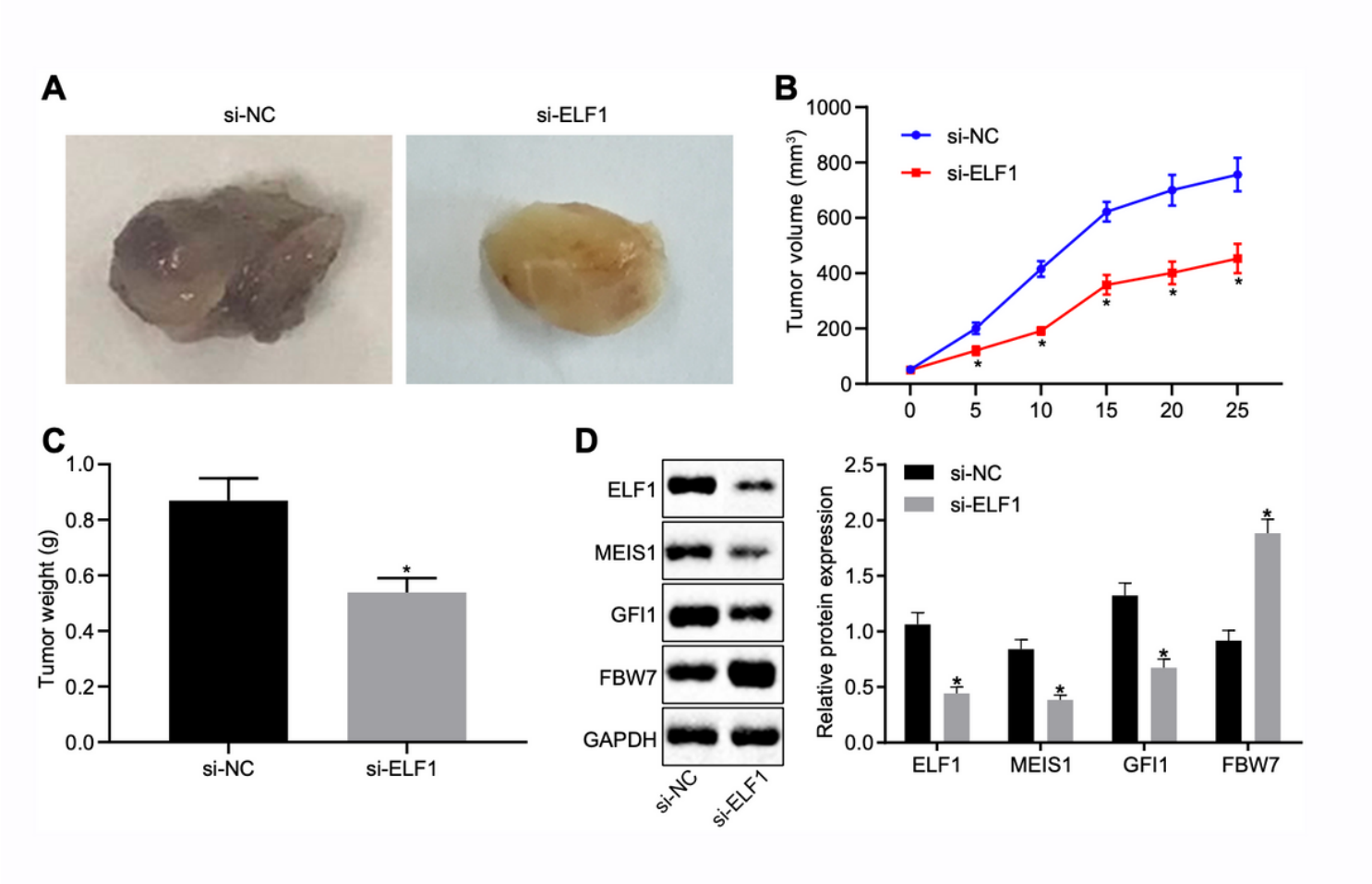

Figure 9

ELF1 inhibited tumor growth in nude mice. A: representative image of tumor formation; B: statistics of tumor volume growth in nude mice; C: tumor weight statistics of nude mice; D: Western-blot was used to detect the expression of related proteins. * represents $p<0.05$. Measurement data were expressed as mean ± standard deviation. un-paired t test was used between the two groups. The method of repeated measurement ANOVA was used for data comparison between groups at different time points. Bonferroni method was used for post-test. n = 8.